short communications

Molecules of *Escherichia coli* MobB assemble into densely packed hollow cylinders in a crystal lattice with 75% solvent content

S. Erumbi Rangarajan,[a] Ante Tocilj,[b] Yunge Li,[b] Pietro Iannuzzi,[a,b] Allan Matte[b] and Miroslaw Cygler[a,b]*

[a]Department of Biochemistry, McGill University, Canada, and [b]Biotechnology Research Institute, National Research Council of Canada and Montreal Joint Centre for Structural Biology, Montreal, Quebec, Canada

Correspondence e-mail: mirek@bri.nrc.ca

The crystal structure of *Escherichia coli* MobB, an enzyme involved in the final step of molybdenum-cofactor biosynthesis, forms intertwined dimers. Each molecule consists of two segments and requires the second monomer for stable folding. Dimerization buries a quarter of the solvent-accessible area of the monomer. These dimers assemble into a hexagonal lattice with $P6_422$ symmetry and occupy only ~25% of the unit-cell volume. The symmetry-related dimers associate tightly into a helical structure with a diameter of 250 Å and a pitch of 98 Å. Two such helices are intertwined, shifted by 49 Å along the sixfold axis. Within the crystal, these helices form thin-walled cylinders with an external diameter of 250 Å and an internal diameter of 190 Å. Their center is filled with solvent. These cylinders pack closely together, forming a hexagonal lattice with the highest possible packing density. This arrangement of dimers allows extensive intermolecular contacts with 75% solvent content in the crystal.

1. Introduction

The involvement of molybdenum, in the form of molybdenum cofactor (Moco), in the metabolism of nitrogen, carbon and sulfur by redox-active enzymes has been well studied. In all enzymes containing Mo or W, with the exception of nitrogenase, molybdopterin (MPT) is found as an invariant component (Rajagopalan, 1991). The synthesis of Moco involves genes from several loci: *moa*, *mob*, *mod*, *moe* and *mog*. In the first step, guanine nucleotide is converted into a derivative precursor termed Z (*moaA*, *moaB*, *moaC*), followed by its conversion to molybdopterin (*moaD*, *moaE*, *moeB*) and subsequently to Moco and molybdopterin guanine dinucleotide (*modA–D*, *mogA*, *mobA*, *mobB*) (Schindelin *et al.*, 2001; Mendel & Schwarz, 2002). In prokaryotes, the active form of the cofactor is MPT modified by attachment to a dinucleotide, either GMP, CMP, AMP or IMP (Rajagopalan & Johnson, 1992). The last step, attachment of the guanine dinucleotide to MPT, is believed to be carried out by MobB (Mendel & Schwarz, 2002). The structure of MobB was reported recently (McLuskey *et al.*, 2003) from two crystal forms belonging to space groups $P2_1$ (1.9 Å resolution) and $P6_422$ (2.4 Å resolution). We have independently obtained crystals of MobB in the hexagonal space group and solved its structure by the multiple anomalous diffraction (MAD) method. The solvent content of these crystals is very high (75%). We therefore analyzed the packing of molecules and describe here the association of molecules of MobB into hollow cylinders with an external

diameter of 250 Å and an internal diameter of 190 Å that are tightly packed in this hexagonal crystal form. Similar or even somewhat higher solvent contents have been observed in other protein crystal structures and are usually associated with high symmetry. Some other examples of protein crystals with high solvent contents and high symmetry are *Escherichia coli* cytidine deaminase (PDB code 1ctt; Betts *et al.*, 1994) and *E. coli* proline-specific aminopeptidase (PDB code 1az9; Wilce *et al.*, 1998).

2. Materials and methods

The gene encoding *E. coli* MobB was cloned into a derivative of pET15b and expressed as a His-tagged, selenomethionine-labeled protein in *E. coli* strain DL41, which is auxotrophic for methionine. The protein was purified following an established protocol (Schrag *et al.*, 2001). The His$_6$ tag was not removed, resulting in an eight-amino-acid extension at the N-terminus of MobB. Crystals were obtained by the hanging-drop vapor-diffusion method. Drops containing 1 µl of protein (7.0 mg ml^{-1}) in buffer [50 m*M* Tris pH 7.5, 200 m*M* NaCl, 5 m*M* DTT and 5%(*v*/*v*) glycerol] and 1 µl reservoir solution consisting of 1.68 *M* ammonium sulfate, 0.5 *M* malonic acid pH 4.5, 15 m*M* acetyl ammonium bromide, 10 m*M* MgCl$_2$ and 1 m*M* β-mercaptoethanol were suspended over 1 ml of reservoir solution. Prior to data collection, the crystals were immersed for 1 min in reservoir solution containing 25%(*v*/*v*) glycerol for cryoprotec-

tion and were flash-cooled to 100 K in a cold stream of N_2 gas. The crystals belonged to space group $P6_422$, with unit-cell parameters $a = 239.0$, $c = 49.1$ Å, $\gamma = 120°$. During the process of structure determination, there were found to be only two molecules in the asymmetric unit, with a resulting solvent content of 75% and a Matthews coefficient of 4.78 $Å^3$ Da^{-1}.

The structure of MobB was determined by MAD phasing from an SeMet-labeled protein crystal (Table 1). Data processing and scaling were performed with *HKL*2000 (Otwinowski & Minor, 1997). All ten Se sites in the asymmetric unit were found with the program *SOLVE* (Terwilliger & Berendzen, 1999) using data to 2.9 Å resolution (overall figure of merit of 0.61). Density modification with the program *RESOLVE* (Terwilliger, 2002) improved the quality of the map. Approximately 45% of the protein main-chain atoms and 20% of the side-chain atoms were built automatically with *RESOLVE*. Further model building was carried out using the program *O* (Jones *et al.*, 1991). The complete model was refined against the remote data set using *CNS* v.1.0 (Brünger *et al.*, 1998). During the refinement, 10% of reflections were set aside in order to monitor R_{free}. Water molecules were added in the last stage of refinement. The crystals of MobB were soaked in a solution containing 5 m*M* GDP and their structure was determined and refined. No electron density for GDP could be found. The final model has a working R factor of 0.276 and an R_{free} of 0.308 for data to 2.8 Å with a sigma cutoff $I > \sigma(I)$, and an R value of 0.305 and an R_{free} of 0.337 for all reflections. The model contains residues Met1–Met43 and Asp51–Asn169, 55 water molecules and two sulfate ions. Residues 44–50 and the C-terminal Gln170 are disordered in both monomers and were located in the electron-density maps. The model has good stereochemistry with no outliers in the Ramachandran plot as analyzed using the program *PROCHECK* (Laskowski *et al.*, 1993).

3. Results and discussion

3.1. Overall structure

Each molecule of MobB is folded into two distinct segments that require interactions with the second monomer for stable folding. The first segment contains six β-strands and three α-helices (residues 1–43 and 80–169) and the second is a two β-strand hairpin followed by one α-helix (residues 51–79). The segment 44–50 is poorly ordered and

Table 1
Data-collection and refinement statistics.

Data set	Inflection	Peak	Remote	Native
Data collection				
Resolution range (Å)	30–2.9	30–2.9	30–2.9	30–2.8
Wavelength (Å)	0.97936	0.97960	0.964368	1.54
Observed reflections	222708	247218	215245	241509
Unique reflections	18439	18469	19110	20053
Completeness (%)	99.5 (96.2)	99.7 (98.7)	99.1 (94.5)	98.5 (87.5)
$I/\sigma(I)$	13.3	13.3	11.4	4.9
R_{sym}† (%)	0.062 (0.199)	0.077 (0.201)	0.086 (0.291)	0.183 (0.716)
Refinement and quality				
Resolution range‡ (Å)			30–2.9	30–2.8
R_{free}§ (No. reflections)			0.327 (1546)	0.308 (1545)
R factor¶ (No. reflections)			0.281 (14392)	0.275 (14120)
R.m.s.d. bonds (Å)			0.009	0.009
R.m.s.d. angles (°)			1.5	1.6
Average B factors ($Å^2$) (No. atoms)				
Main-chain atoms				
Monomer A			26.2 (647)	26.7 (647)
Monomer B			46.5 (647)	47.1 (647)
Side-chain atoms				
Monomer A			30.4 (624)	30.9 (624)
Monomer B			50.6 (624)	51.1 (624)
Water			21.4 (55)	21.9 (55)
Sulfate			59.7 (2)	60.0 (2)
Ramachandran plot: % residues in				
Most favorable regions			70.8	68.2
Additional allowed regions			25.4	27.7
Generously allowed regions			3.4	4.10
Disallowed regions			0.4	0.0

† $R_{sym} = \sum |I_{obs} - I_{avg}|/\sum I_{avg}$.   ‡ Refinement performed using data collected at the remote wavelength with $I > \sigma(I)$.   § R_{free} is the same as R_{work}, but for a random set of 10% of the unique reflections.   ¶ $R = \sum |F_{obs} - F_{calc}|/\sum F_{obs}$.
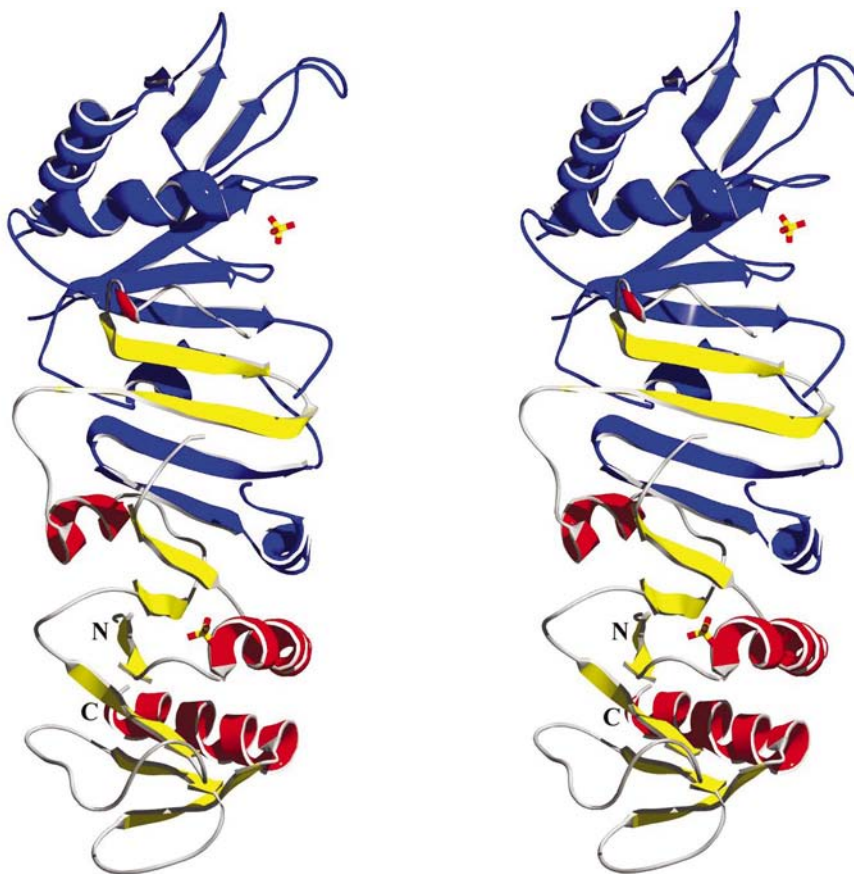

Figure 1
Ribbon diagram of the MobB dimer. Molecule A is depicted with strands colored yellow, helices red and loops gray; molecule B is colored blue. The two sulfate ions bound to the dimer are shown explicitly. The figure was created with *sPDBv* (Guex & Peitsch, 1997) and *POV-Ray* (http://www.povray.org).

was not modeled. The crystal structure shows that the two molecules of MobB are intertwined and form an extensive 16-stranded β-sheet with a nearly 180° twist. Six of the eight α-helices are located on topologically the same side of the β-sheet. The pseudo-twofold axis relating the two monomers is perpendicular to the plane of the sheet. Within the β-sheet, the first six parallel β-strands are from monomer 1 (M1), the following hairpin of two β-strands is from monomer 2 (M2), the next two β-strand hairpins are from M1 and the last six parallel β-strands are from M2 (Fig. 1). The first six and the last six β-strands are antiparallel to each other but point in the same direction owing to the twist of the β-sheet. This interdigitation of the two monomers indicates that the folding unit of MobB is a dimer. One side of the dimer is concave and the other convex. The dimer is elongated, with dimensions of 90 × 37 × 28 Å. The two monomers superimpose with a root-mean-square (r.m.s.) deviation of 1.0 Å for all C^{α} atoms and 1.6 Å for all atoms.

The extent of the interactions between the two monomers is exemplified by the fact that 85 of the 157 well ordered residues of one molecule are within 4 Å of atoms from the second monomer. The buried surface area is ~2270 Å^2 per monomer. This accounts for ~25% of the total surface area. The present model of MobB agrees well with that obtained by McLuskey *et al.* (2003) (PDB code 1np6) at a higher resolution, giving an r.m.s.d. of ~1.0 Å for the C^{α} atoms when either of the two independent monomers are compared. The arrangement of the dimer is also well maintained in the two different space groups and packing modes, with an r.m.s.d. of 1.2 Å for 300 C^{α} atoms of the dimer. Most of the residues in the two models have similar side-chain orientations; however, several regions of chain *B* (Gly12–Gly14, His38–Asp42, Asp51–Ser52) show different conformations in the two dimers which are likely to result from differences in crystal contacts. The sulfate ion in monomer *A* is the same in our structure and in 1np6 (separation of 0.8 Å after superposition of the dimers), while the sulfates bound to monomer *B* differ in position by 2.9 Å. This shift is associated with a difference in the conformation of loop Ser11–Gly14 to which the sulfate ion binds.

3.2. Crystal packing

Despite a solvent content of 75% and the associated unusually high Matthews coefficient of 4.8 Å^3 Da^{-1}, the hexagonal crystals
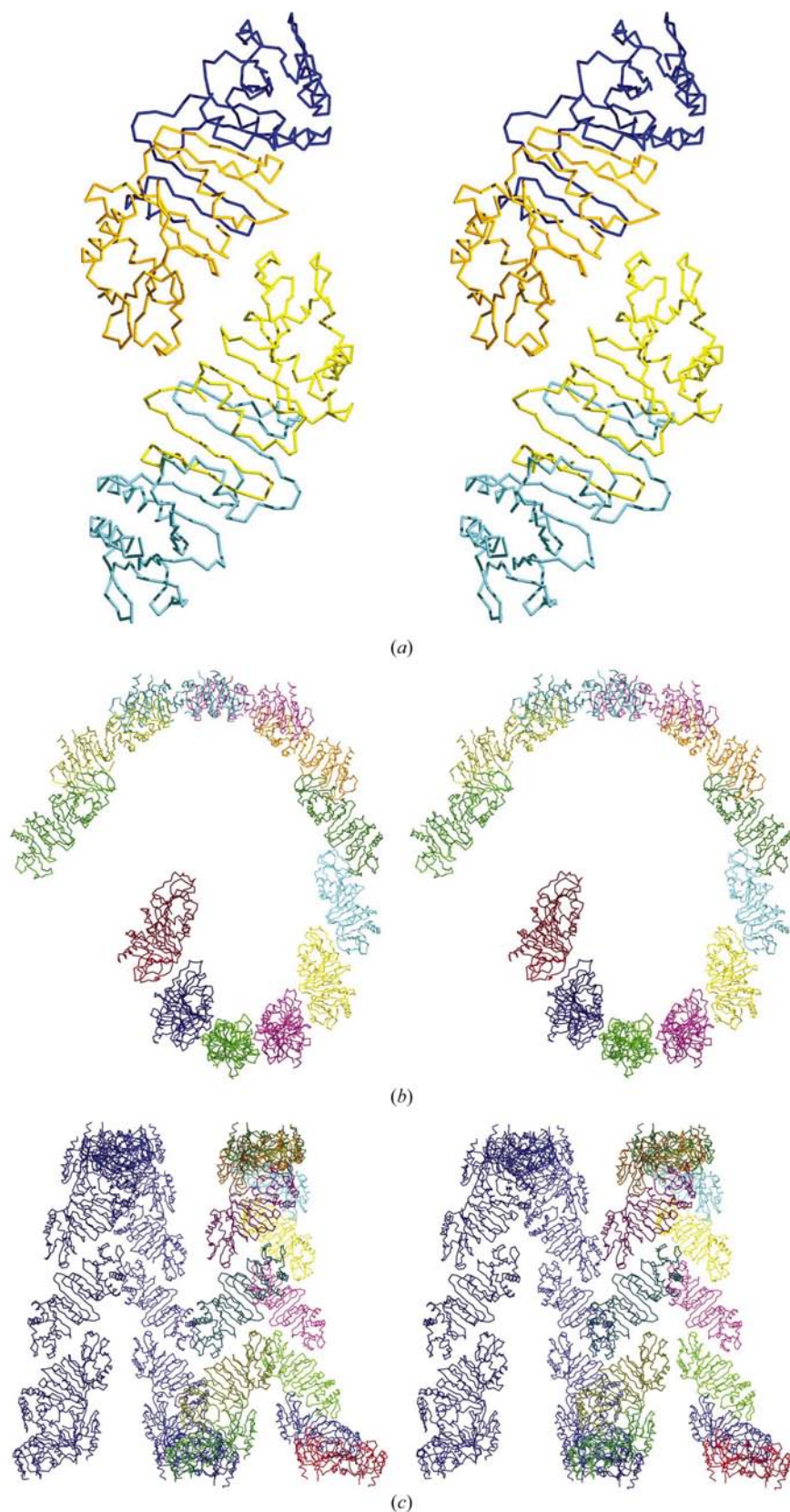

Figure 2
Crystal packing of MobB in the *P*6$_4$22 space group. (*a*) The tetramer created by the application of twofold symmetry. Molecules *A* are colored yellow and orange and molecules *B* cyan and blue. (*b*) Six tetramers (12 dimers) related by the 6$_4$ symmetry and forming one turn of a helix. Each dimer is colored a different color. (*c*) Two turns of the same continuous helix are shown.

of MobB diffract to medium resolution. Crystals grown in our laboratory diffracted to 2.8 Å resolution and McLuskey *et al.* (2003) reported 2.4 Å resolution from the same crystal form. Therefore, we investigated the packing of MobB molecules in the crystal in order to gain an understanding of the reasons for such relatively good diffraction. Inspection of the electron-density map as well as comparison of the temperature factors showed that molecule A ($\langle B$ factor$\rangle = 29$ Å^2) within the dimer is better ordered than molecule B ($\langle B$ factor$\rangle = 49$ Å^2) (Table 1). The $6_4 22$ symmetry creates 12 symmetry-related dimers. Transformation along the twofold axis creates a tetramer

(Fig. 2a). This tetramer is replenished by the 6_4 symmetry axis into one turn of a helix made of 12 dimers (Fig. 2b). The pitch of this helix is $2 \times c$ axis = 98.2 Å (Fig. 2c), with the contacts between molecules occurring only along the circumference of the helix. Two such helices are intertwined, forming a solid surface with the interactions between the molecules along the direction of the helix axis (the crystallographic z axis) shown in Fig. 2(d). Viewed along the helix axis, this arrangement creates a hollow cylinder with an external diameter of 250 Å and a wall thickness of ∼30 Å. In the unit cell, these cylinders are arranged in dense hexagonal packing with the highest possible packing

density, corresponding to dense packing of spheres in a plane (Fig. 2e). The contacts between the cylinders are formed by interactions between the middle and C-terminal segments of molecule A of each dimer, while the B molecules have a large solvent-exposed area. This arrangement therefore provides an explanation for the higher mobility displayed by molecule B compared with molecule A.

There are two types of solvent channel in the crystal. Large 190 Å diameter solvent channels run down the center of each cylinder. Smaller triangular cross-section channels run between three touching cylinders, with their centers at the crystallographic coordinates (1/3, 2/3, 0) and (2/3, 1/3, 0). The disordered segment of each molecule, residues 44–50, is on the surface of the dimer facing the large solvent channel on the internal surface of the cylinder.

3.3. Substrate-binding site

Although the precise function of MobB has not yet been identified, it is postulated that it takes part in the transfer of a guanine dinucleotide moiety to molybdopterin in the final step of MGD synthesis (Mendel & Schwarz, 2002). Eaves *et al.* (1997) have shown that MobB can bind GTP (K_M of 7.5 µM) and also exhibits very weak GTPase activity. The alignment of MobB sequences from 49 species (PFAM 03205, http://www.sanger.ac.uk/Software/Pfam/) shows the location of highly conserved residues. When mapped onto the structure of MobB, these residues occur on the concave side of the dimer and are exposed in the central solvent channel. The substrate-binding site is expected to be located near these highly conserved amino acids and should therefore be accessible in the crystal. A sulfate ion is present in the P-loop region of each monomer, the putative nucleotide triphosphate binding site in which the phosphoryl groups are expected to bind. This putative substrate-binding site is discussed in detail by McLuskey *et al.* (2003). However, neither soaking nor co-crystallization experiments with GDP or the non-hydrolysable GTP homolog GTPγS showed density for this molecule. These results suggest that binding of GTP might require prior binding of the MPT molecule or that interaction with another protein is needed to conclude the reaction. *In vivo* experiments that disrupted several genes in the MPT synthesis pathway suggested that MobB interacts with MobA and MoeA (Magalon *et al.*, 2002). McLuskey *et al.* (2003) have modeled possible interactions between MobB and MobA.
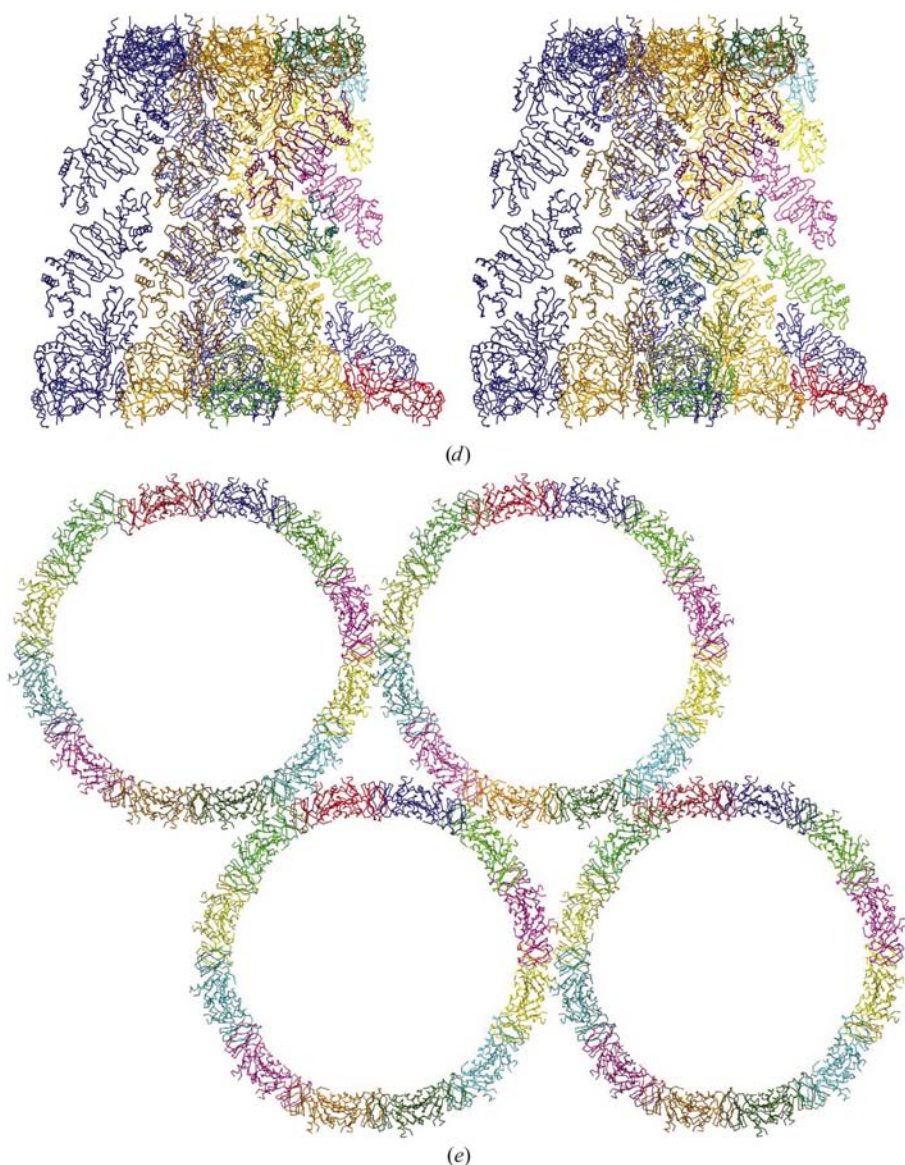

Figure 2 (continued)
Crystal packing of MobB in the $P6_4 22$ space group. (d) Two intertwined helices forming a cylinder with tightly packed walls. Each helix is shown in a unique color. (e) View along the z axis corresponding to the axis of the cylinder. The cylinders are arranged in dense hexagonal packing. The large solvent channels are inside the cylinders and the smaller channels are between three cylinders.

Attempts in our laboratory to crystallize the MoeA–MobB complex alone and in the presence of GDP or GTPγS were unsuccessful.

References

Betts, L., Xiang, S., Short, S. A., Wolfenden, R. & Carter, C. W. Jr (1994). *J. Mol. Biol.* **235**, 635–656.

Brünger, A. T., Adams, P. D., Clore, G. M., DeLano, W. L., Gros, P., Grosse-Kunstleve, R. W., Jiang, J.-S., Kuszewski, J., Nilges, M., Pannu, N. S., Read, R. J., Rice, L. M., Simonson, T. & Warren, G. L. (1998). *Acta Cryst.* D**54**, 905–921.

Eaves, D. J., Palmer, T. & Boxer, D. H. (1997). *Eur. J. Biochem.* **246**, 690–697.

Guex, N. & Peitsch, M. C. (1997). *Electrophoresis*, **18**, 2714–2723.

Jones, T. A., Zhou, J. Y., Cowan, S. W. & Kjeldgaard, M. (1991). *Acta Cryst.* A**47**, 110–119.

Laskowski, R. A., MacArthur, M. W., Moss, D. S. & Thornton, J. M. (1993). *J. Appl. Cryst.* **26**, 283–291.

McLuskey, K., Harrison, J. A., Schuttelkopf, A. W., Boxer, D. H. & Hunter, W. N. (2003). *J. Biol. Chem.* **278**, 23706–23713.

Magalon, A., Frixon, C., Pommier, J., Giordano, G. & Blasco, F. (2002). *J. Biol. Chem.* **277**, 48199–48204.

Mendel, R. R. & Schwarz, G. (2002). *Met. Ions. Biol. Syst.* **39**, 317–368.

Otwinowski, Z. & Minor, W. (1997). *Methods Enzymol.* **276**, 307–326.

Rajagopalan, K. V. (1991). *Adv. Enzymol. Relat. Areas Mol. Biol.* **64**, 215–290.

Rajagopalan, K. V. & Johnson, J. L. (1992). *J. Biol. Chem.* **267**, 10199–10202.

Schindelin, H., Kisker, C. & Rajagopalan, K. V. (2001). *Adv. Protein Chem.* **58**, 47–94.

Schrag, J. D., Huang, W., Sivaraman, J., Smith, C., Plamondon, J., Larocque, R., Matte, A. & Cygler, M. (2001). *J. Mol. Biol.* **310**, 419–431.

Terwilliger, T. C. (2002). *Acta Cryst.* D**58**, 1937–1940.

Terwilliger, T. C. & Berendzen, J. (1999). *Acta Cryst.* D**55**, 849–861.

Wilce, M. C., Bond, C. S., Dixon, N. E., Freeman, H. C., Guss, J. M., Lilley, P. E. & Wilce, J. A. (1998). *Proc. Natl Acad. Sci. USA*, **95**, 3472–3477.